

Viscoelastic Properties and Creep-Fatigue Behavior of PA2200/HA Composites Manufactured by Selective Laser Sintering

F. Dabbas¹, S. L. Stares², H. Schappo¹, D. Hotza² and G. V. Salmoria¹

1. *Innovation Laboratory for Molding and Additive Manufacturing (NIMMA), Federal University of Santa Catarina (UFSC), Florianópolis 88040-900, SC, Brazil*

2. *Interdisciplinary Laboratory for the Development of Nanostructures (LINDEN), Federal University of Santa Catarina (UFSC), Florianópolis 88040-900, SC, Brazil*

Abstract: Porous (polyamide/hydroxyapatite) composites were manufactured via SLS (selective laser sintering) process. Specimens with different PA2200/HA contents (100/0; 95/5; 90/10 and 80/20) were sintered at relative low laser energy density. The porous composite specimens were characterized for dynamic-mechanical analysis. The dynamic-mechanical properties changed as a function of the composition of the composite materials. Storage and loss modulus vary from 1,050 to 215 MPa and 35 to 5 MPa, respectively.

Key words: Composite biomaterials, polyamide/hydroxyapatite, SLS.

1. Introduction

SLS (selective laser sintering) is an additive manufacturing process that creates 3D parts by the sintering of powdered materials, layer-by-layer, using infrared laser beams [1]. The level of control over the microstructure and mechanical properties of SLS parts is dependent on the process parameters, particularly powder composition, laser power and scan speed [2, 3]. Previous works have demonstrated that SLS has potential to construct custom-made implants and synthetic body parts like bones and organs [4-6]. However, the variety of commercial materials available for the SLS process is restricted and this reduces the options during the selection of material for the manufacturing of parts. The use of a non-commercially material can increase the range of

properties of the SLS parts.

Bioceramics like HA (hydroxyapatite) have been given a lot of attention as candidate materials to be used in bone repair situations because they possess highly desirable characteristics like biocompatibility and osteoconductivity [7, 8]. PA (polyamide) also is biocompatible and can offer advantages related to the low processing temperatures and high corrosion resistance in comparison to other materials [9, 10]. So a composite material may be done in such a way that the final product may acquire some excellent properties that cannot be found individually in either material [11].

In a previous work, Zhang and coauthors [12] provided comparative results between fully dense and SLS specimens. In this work, the recovery and fatigue properties of PA2200/HA composites manufactured by SLS were further investigated. The influence of material compositions on the mechanical properties of the manufactured specimens is discussed.

Corresponding author: Dachamir Hotza, Dr.-Ing., professor, research fields: processing of materials and composites.

2. Experimental

2.1 Materials

The polymeric powder used in this study was commercial polyamide PA2200 (EOSINT) with average particle size of 60 μm . The HA (FLUKA-Assay 90%) mean particle size used was 5 μm . The HA contents in the composites were 0, 5, 10 and 20 wt.%. The composites were prepared with a Y mixer for a period of 2 h.

2.2 SLS

Composite specimens with dimension of 35 mm long \times 5 mm wide \times 1.4 mm thick were manufactured. The PA2200/HA specimens consisted of nine selective laser sintered layers with 150 μm layer thickness of powder deposition. Using an RF-excited CO₂ laser, with a wavelength of 10.6 μm , laser beam diameter of 250 μm , scan speed of 57 $\text{mm}\cdot\text{s}^{-1}$ and chamber temperature of 140 $^{\circ}\text{C}$, the initial properties of the specimens manufactured are listed in Table 1. These parameters were selected in a previous work [13] with the target to obtain samples with an adequate degree of sintering for our applications.

2.3 SEM (Scanning Electron Microscopy)

The composite specimens were observed under a Phillips XL30 SEM in order to investigate the fracture surface, particle aspects and microstructure. The specimens were coated with gold in a Bal-Tec Sputter Coater SCD005.

2.4 Mechanical Tests

Dynamic-mechanical analysis was performed (TA Instruments, model Q800) with single cantilever mode.

Stress-strain curves were obtained at a strain rate of 2 $\text{mm}\cdot\text{min}^{-1}$ and 30 $^{\circ}\text{C}$. The storage modulus (E') and the loss modulus ($\tan\delta = E''/E'$) at a fixed frequency of 1 Hz were determined in a temperature range of -10 to 200 $^{\circ}\text{C}$ with a heating rate of 3 $^{\circ}\text{C}\cdot\text{min}^{-1}$. Creep-recovery data were obtained at 30 $^{\circ}\text{C}$ by applying the equivalent of 50% of the maximum strain amplitude of the previously obtained stress-strain curves for each specimen for 20 min. The recovery was then evaluated for 35 min. Fatigue experiments were conducted at 30 $^{\circ}\text{C}$ and 1 Hz by applying 50% of the maximum strain amplitude determined in the stress versus strain curves for each specimen.

3. Results and Discussion

Fig. 1 shows representative images of the fractured surface of PA2200/HA specimens with compositions of 95/5, 90/10 and 80/20 after the SLS process. The PA particles were observed to have good interparticle bonding and the HA particles are heterogeneously distributed between the PA matrix. In addition, a low chemical affinity was observed between the PA and HA phases. Higher weight percentage of HA means less binder and consequently less material to fuse and facilitate composite particulate bonding [10, 14].

Fig. 2 shows the behavior of the storage modulus (E'), as a function of temperature for PA2200 and PA2200/HA specimens. Pure PA2200 initially showed a slight decrease in the E' values up to 20 $^{\circ}\text{C}$ followed by a sharper decrease up to 62 $^{\circ}\text{C}$. Above 62 $^{\circ}\text{C}$, E' presented a smaller decrease with an increase in temperature until its melting point 181 $^{\circ}\text{C}$. The E' values for the PA2200/HA specimens were lower than those for the pure PA2200. The E' value for the 80/20 samples was the lowest (215 MPa at 0 $^{\circ}\text{C}$)

Table 1 Processing parameters and properties of PA/HA composites manufactured by SLS.

PA2200/HA (w/w)	100/0	95/5	90/10	80/20
Energy density (W mm^{-2})	0.281	0.281	0.351	0.351
Porosity (%)	47	51	45	41
Elastic modulus (GPa)	0.38 ± 0.05	0.31 ± 0.08	0.17 ± 0.03	0.12 ± 0.01
Ultimate strength (MPa)	55.7 ± 10	22.2 ± 9	17.7 ± 3	5.2 ± 1

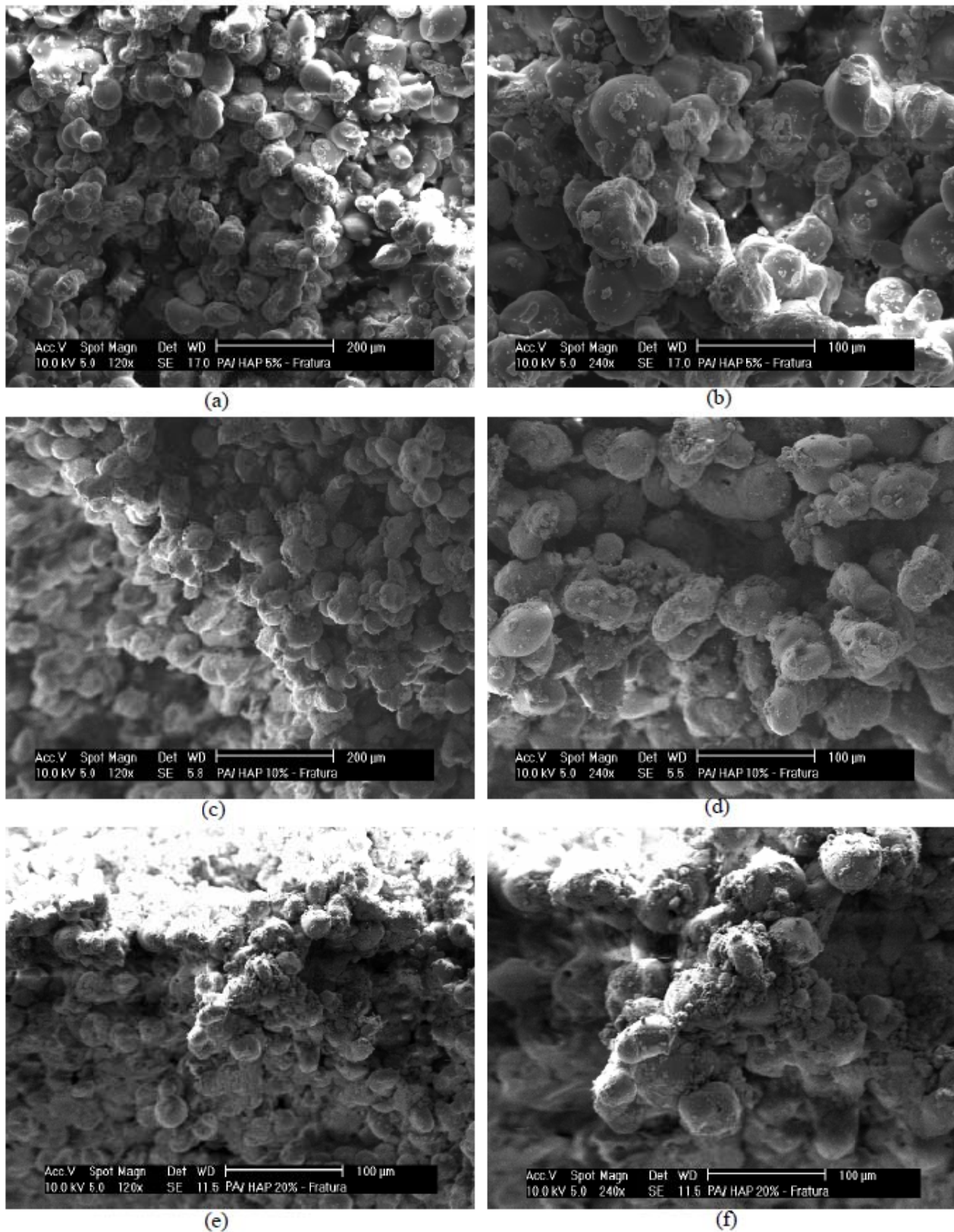


Fig. 1 SEM micrographs of surface fracture: (a)-(b) 95/5, (c)-(d) 90/10 and (e)-(f) 80/20 at 120x and 240x magnifications, respectively.

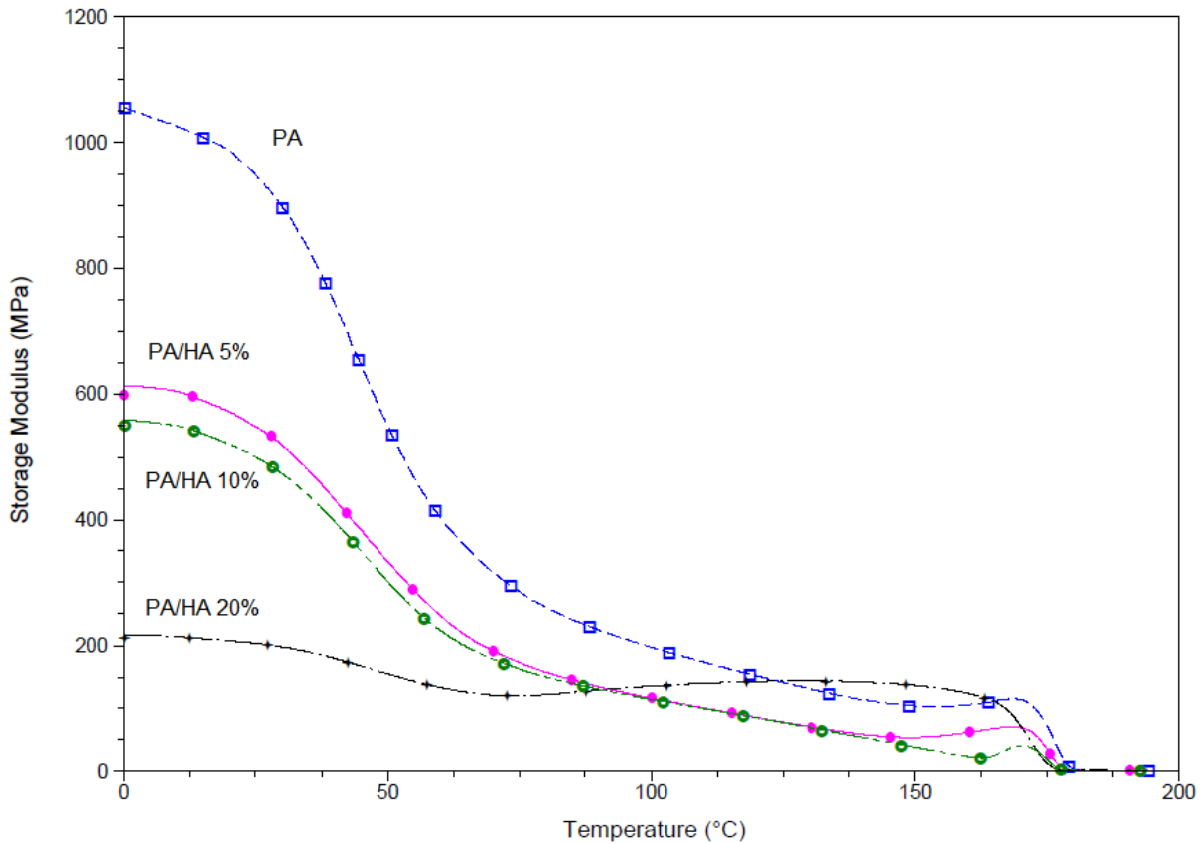


Fig. 2 E' modulus of pure components and PA2200/HA composites as a function of temperature.

and presented a small decrease with increasing temperature up to 20 °C. From 20 °C, the E' value decreased rapidly with temperature up to 62 °C. At higher temperatures, the E' value remained constant up to its melting point 182,5 °C. The 95/5 and 90/10 specimens showed closer and intermediary E' values (560 MPa and 610 MPa, respectively) in relations to pure PA2200 and 80/20 specimens. These last specimens also showed similar behavior to that of pure PA2200, due to the major PA2200 content.

Fig. 3 shows the loss modulus (E'') as a function of temperature for PA2200 and PA2200/HA specimens. PA2200 had a glass transition temperature of 48 °C when $\tan\delta$ reached the maximum (α relaxation). The α relaxation is caused by segmental motion of the chains, relating to the PA2200 amorphous phase. A second relaxation for PA2200 can be observed below the melting point, at 175 °C, which is attributed to the crystalline regions (α_c' relaxation) in polyamides. The maximum value of loss modulus E'' for PA2200 was

approximately 35 MPa. The loss modulus E'' value for the PA2200/HA specimens showed the same transitions (relaxations) observed for the pure components. The relaxation intensity was proportional to the specimen composition.

The recovery test curves in Fig. 4 show the percentage deformation (related to the maximum strain in the stress-strain curves) obtained for each specimen in the creep test as a function of time. When pure PA2200 was deformed to the equivalent of 50% of the maximum strain amplitude, it had 10% of permanent plastic deformation, and 90% of the remaining deformation was recovered through elastic behavior. The composite creep curves demonstrated that 95/05 and 90/10 PA2200/HA specimens had similar plastic and elastic behavior and showed considerable elastic recovery (71%) due to the high quantity of PA2200 in the composite composition. The 80/20 samples showed only 28% of elastic recovery, due to the higher quantity of HA in the composite composition.

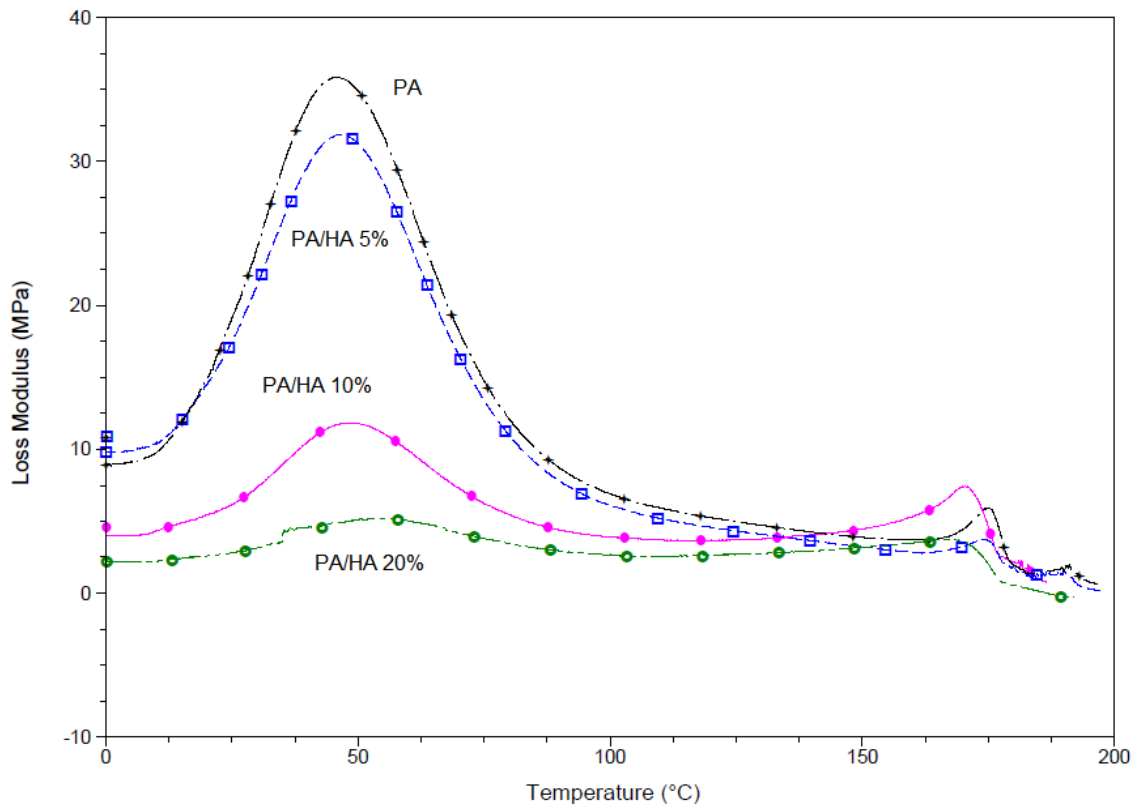


Fig. 3 Loss Modulus (E'') of pure components and PA2200/HA composites as a function of temperature.

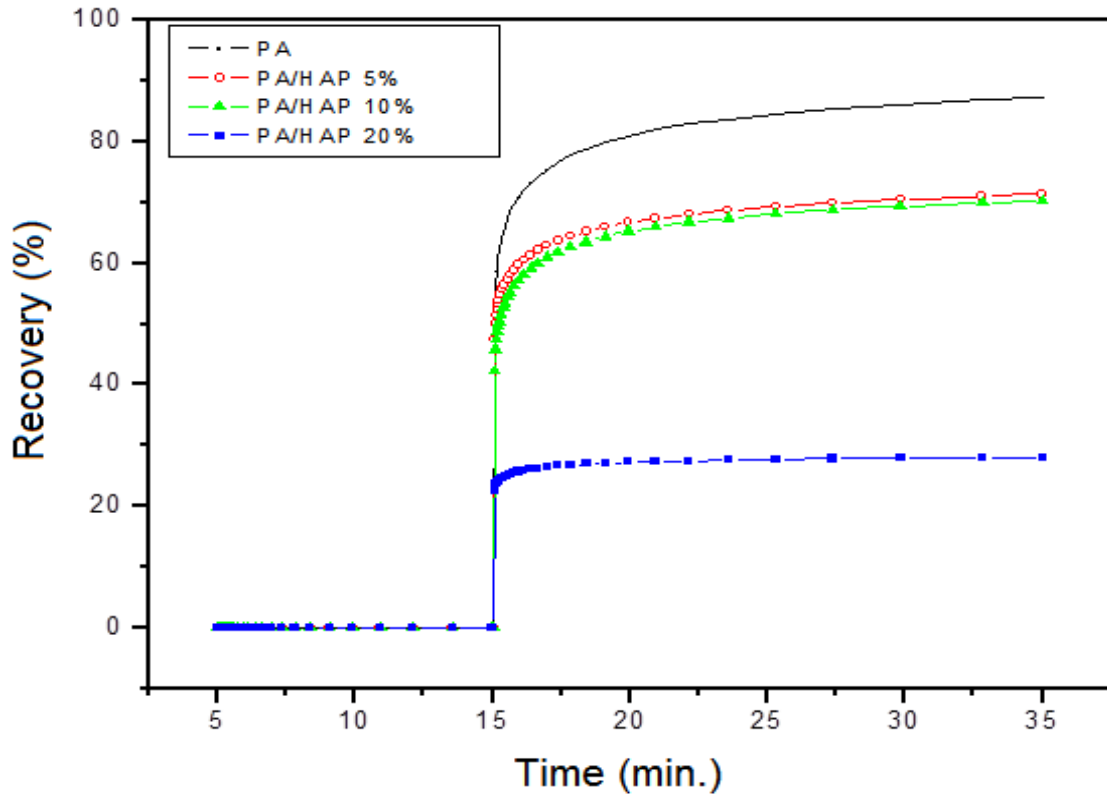


Fig. 4 Creep test curves showing values for strain (%) versus time for the PA2200/HA specimens.

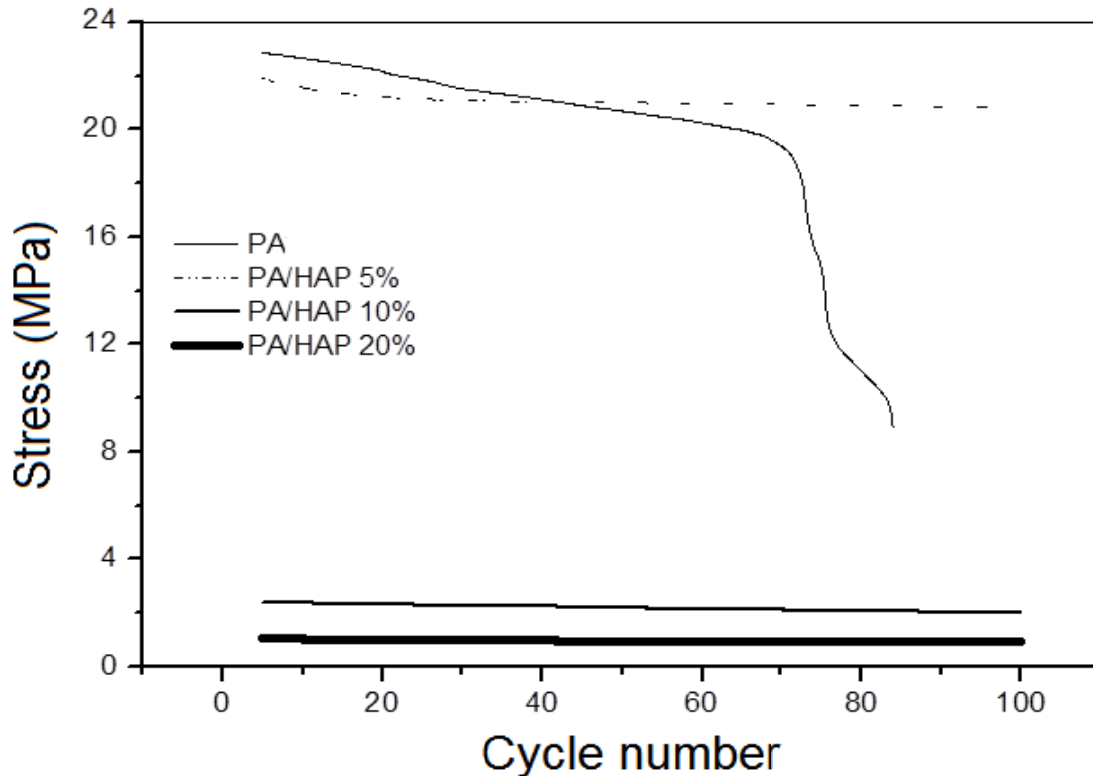


Fig. 5 Fatigue curves showing the values of stress versus cycle number for the pure PA2200 and PA2200/HA specimens.

The fatigue curves showing the stress variation as a function of the number of cycles at 50% of the maximum strain for the pure PA2200 and PA2200/HA specimens are presented in Fig. 5. Pure PA2200 presented a reduction in stiffness (creep phenomenon) and a stress reduction of 10 MPa after 7,000 cycles due to increased shear in the $-CH_2-$ group segments leading to rapid failure under the test conditions [15, 16]. On the other hand, the fatigue behavior of the HA composites remained stable for the 3 types of PA2200/HA specimens. Stress value of 95/05 PA2200/HA specimen was in the same order of pure PA2200, due to the major PA matrix ratio which provided greater strength and stiffness. The 90/10 and 80/20 composite specimens showed lower fatigue strength and more laser power for sintering. The low stress values of the 80/20 and 90/10 composite specimens indicate the low chemical affinity between the PA2200 and HA phases. Higher weight percentage of HA means less binder and consequently less material to fuse and facilitate composite particulate

bonding. In contrast to the literature [17, 18], in this work the increase of laser power did not promote the increase on the mechanical properties of sintered specimens, as expected by the fact that higher energy density levels cause a better fusion of the powder particles, resulting in a more solid part being formed. The effect of HA content was more significant than the effect of laser power, resulting from decrease of mechanical properties.

4. Conclusions

PA2200/HA specimens were successfully manufactured using SLS process and it was possible to control their structures and properties by the adjusting of composition. The microstructures of composites specimens were heterogeneous with low chemical affinity between the PA and HA phases. The mechanical testing of PA2200/HA composites showed that the behavior of the E' modulus varied according to the proportion of HA component in the specimens composition. The creep test showed that specimens

with lower amount of HA had greater plastic deformation. In the fatigue test, all composite specimens presented no changes in their behavior and the 90/10 and 80/20 samples presented low fatigue strength under the test conditions.

References

- [1] Zocca, A., Colombo, P., Gomes, C. M., and Guenster, J. 2015. "Additive Manufacturing of Ceramics: Issues, Potentialities, and Opportunities." *J. Am. Ceram. Soc.* 98: 1983-2001.
- [2] Salmoria, G. V., Ahrens, C. H., Klaus, P., Paggi, R. A., Oliveira, R. G., and Lago, A. 2007. "Rapid Manufacturing of Polyethylene Parts with Controlled Pore Size Gradients Using Selective Laser Sintering." *Mater. Res.* 10: 211-4.
- [3] Salmoria, G. V., Leite, J. L., and Paggi, R. A. 2009. "The Microstructural Characterization of PA6/PA12 Blend Specimens Fabricated by Selective Laser Sintering." *Polym. Test.* 28: 746-51.
- [4] Feng, P., Niu, M., Gao, C., Peng, S., and Shuai, C. 2014. "A Novel Two-Step Sintering for Nano-Hydroxyapatite Scaffolds for Bone Tissue Engineering." *Sci. Rep.* 4: 5599-609.
- [5] Liu, F. H. 2014. "Synthesis of Biomedical Composite Scaffolds by Laser Sintering: Mechanical Properties and *in Vitro* Bioactivity Evaluation." *Appl. Surf. Sci.* 297: 1-8.
- [6] Savalani, M. M., Hao, L., Zhang, Y., Tanner, K. E., and Harris, R. A. 2007. "Fabrication of Porous Bioactive Structures Using the Selective Laser Sintering Technique." *P. I. Mech. Eng. H* 221: 873-86.
- [7] Liu, F. H., Shen, Y. K., and Lee, J. L. 2012. "Selective Laser Sintering of a Hydroxyapatite Silica Scaffold on Cultured MG63 Osteoblasts *in Vitro*." *Int. J. Precis. Eng. Man.* 13: 439-44.
- [8] Rezwani, K., Chen, Q. Z., Blaker, J. J., and Boccaccini, A. R. 2006. "Biodegradable and Bioactive Porous Polymer/Inorganic Composite Scaffolds for Bone Tissue Engineering." *Biomaterials* 27: 3413-31.
- [9] Childs, T. H. C., Berzins, M., Ryder, G. R., and Tontowi, A. E. 1999. "Selective Laser Sintering of an Amorphous Polymer—Simulations and Experiments." *P. I. Mech. Eng. B-J Eng.* 213: 333-49.
- [10] Savalani, M. M., Hao, L., Dickens, P. M., Zhang, Y., Tanner, K. E., and Harris, R. A. 2012. "The Effects and Interactions of Fabrication Parameters on the Properties of Selective Laser Sintered Hydroxyapatite Polyamide Composite Biomaterials." *Rapid. Prototyping J.* 18: 16-27.
- [11] Stares, S. L., Fredel, M. C., Aragonés, A., Gutmanas, E. Y., Gotman, I., Greil, P., and Travitzky, N. 2013. "PLLA/HA Composite Laminates." *Adv. Eng. Mater.* 15: 1122-4.
- [12] Zhang, Y., Hao, L., Savalani, M. M., Harris, R. A., and Tanner, K. E. 2008. "Characterization and Dynamic Mechanical Analysis of Selective Laser Sintered Hydroxyapatite-Filled Polymeric Composites." *J. Biomed. Mater. Res. A* 3: 607-16.
- [13] Dabbas, F., Stares, S. L., Hotza, D., and Salmoria, G. V. 2017. "Selective Laser Sintering of Polyamide/Hydroxyapatite Scaffolds." In *Proceedings of the 3rd Pan American Materials Congress*, 95-103. doi: 10.1007/978-3-319-52132-9_10.
- [14] Beal, V. E., Paggi, R. A., Salmoria, G. V., and Lago, A. 2009. "Statistical Evaluation of Laser Energy Density Effect on Mechanical Properties of Polyamide Parts Manufactured by Selective Laser Sintering." *J. Appl. Polym. Sci.* 5: 2910-9.
- [15] Salmoria, G. V., Leite, J. L., Vieira, L. F., Pires, A. T. N., and Roesler, C. R. M. 2012. "Mechanical Properties of PA6/PA12 Blend Specimens Prepared by Selective Laser Sintering." *Polym. Test* 31: 411-6.
- [16] Salmoria, G. V., Leite, J. L., Paggi, R. A., Lago, A., and Pires, A. T. N. 2008. "Selective Laser Sintering of PA12/HDPE Blends: Effect of Components on Elastic/Plastic Behavior." *Polym. Test* 27: 654-9.
- [17] Kruth, J. P., Levy, G., Klocke, F., and Childs, T. H. C. 2007. "Consolidation Phenomena in Laser and Powder-Bed Based Layered Manufacturing." *Man. Tech.* 56: 730-59.
- [18] Goodridge, R. D., Tuck, C. J., and Hague, R. J. M. 2012. "Laser Sintering of Polyamides and Other Polymers." *Prog. Mater. Sci.* 57: 229-67.